



Computational Vision System for Classification and Recognition of Malignant Melanoma using Image Processing and ABCD Rule Techniques

¹S. Raviraja *, ²Manasa. E, ³M. L. Anitha

¹Principal Investigator, Royal Research Foundation, Mysore, Karnataka, India

²M.Tech Student, Department of CS & E, PES College of Engineering, Mandya, Karnataka, India

³Associate Professor, Department of CS & E, PES College of Engineering, Mandya, Karnataka, India

Abstract— *worldwide efforts in identification, prevention and diagnosis for melanoma were more but melanoma continues to rise at alarming state. Several new methods of computer aided Malignant diagnosis have recently been developed, however, all of these are dependent on clinical notion and, consequently on explicit clinical request. Although several methods lend themselves to automation, no technique can yet be used for routine clinical automated screening. The proposed research introduces a skin lesion image processing for detecting malignant features in acquired images from dermatoscopes, in order to evaluate the skin lesion. The main features of malignant melanoma are blue-white veil, numerous brown dots, pseudopodia, radial streaks, and discoloration of a scar, black dots-globules at the periphery, many colors, numerous blue/gray dots and extended network. The aim of the proposed research work is to develop a scientific hybridized model to classify and recognize by means of Image Processing Techniques in analyzing Malignant Melanoma diagnosis. Further evaluation of the size and shape of the Melanocytes also considered. We found that the automated diagnostic detection were able to predict the malignant melanoma with an accuracy of 60-83% based on selected dependent variables, validated using ROC characteristics. The proposed model with variable shows excellent performance with a test value of the ROC of 0.80 and 0.87. ROC can range between 0 and 1 with higher values indicating better performance.*

Keywords— *Skin Cancer, Malignant Melanoma, Dermatoscope, SIAscope Image, Feature Extraction, ABCD Rule.*

I. INTRODUCTION

Melanoma is a disease in which malignant (cancer) cells exist in Melanocytes. There are different types of cancer that occur in the layer of skin. Melanoma can found anywhere on the skin. Melanocytes are Cells that make melanin and are found in the lower part of the epidermis. Melanin is the pigment that gives skin its natural color. When skin is exposed to the sun or artificial light, Melanocytes make more pigment and cause the skin to darken. Melanocytes are in the layer of basal cells at the deepest part of the epidermis.

The number of new cases of melanoma has been increasing over the last 40 years. The lifetime risk of an American developing invasive melanoma in Figure 1.1 illustrates the increasing rates of melanoma from 1930 to 2015. Melanoma is most common in adults, but it is rarely found in children and adolescents. The majority of the melanomas are black or brown, but the melanomas also are skin-colored, pink, red, purple, blue or white. Melanoma occurs mainly by intense, occasional UV exposed (frequently leading to sunburn), especially in those patients with genetically predisposed disease. Melanoma kills an estimated 9,940 people in the US annually. It is a fact that the melanoma is recognized and treated early, it is almost and always curable, or otherwise, the cancer positively advances and spread to other parts of the human body, where it becomes hard to treat and can be fatal. While it is not the most common of the skin cancers, melanoma causes the most deaths. Based on the facts and figures The American Cancer Society estimates that the present scenario is more than 135,000 new cases of melanoma in the US alone are diagnosed every year. Latest statistics around the year 2015 estimated 73,870 of these will be invasive melanomas, with about 42,670 in males and 31,200 in women. In case of men, melanoma is often found on the trunk or the head and neck. In women, melanoma forms most often on the arms and legs. When melanoma occurs in the eye, it is called intraocular or ocular melanoma.

The American Cancer Society's estimates for melanoma in the United States from 2000 to 2011 is shown in Figure 1.2 in which about 58% melanomas in men and 42% melanomas in women will be diagnosed (about 276,968 in men and 199,796 in women). The risk of melanoma increases as people age. The average age of people when it is diagnosed is 63. But melanoma is not uncommon even among those younger than 30. The American Cancer Society's estimates Age distribution for melanoma from 2000-2011 in the United States is depicted in Figure 1.3.

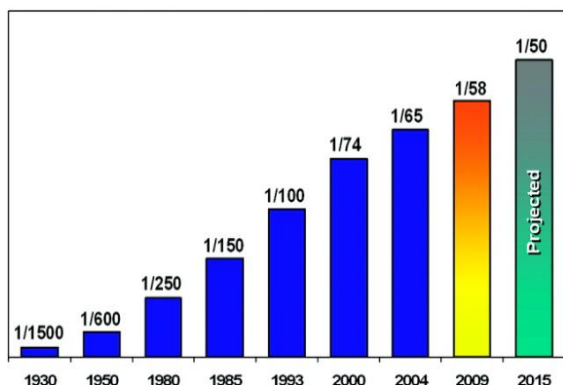


Fig 1.1 Lifetime risk of an American developing invasive melanoma

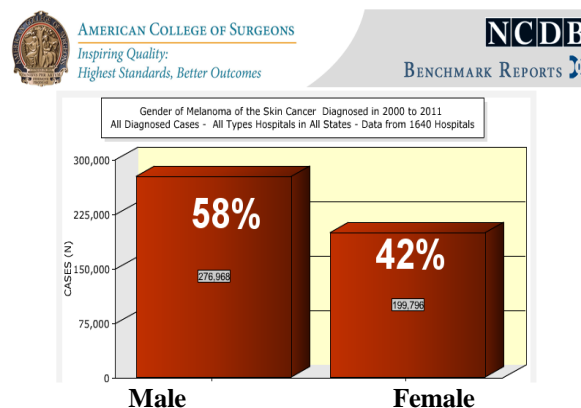


Fig 1.2 Melanoma – Gender Distribution - USA

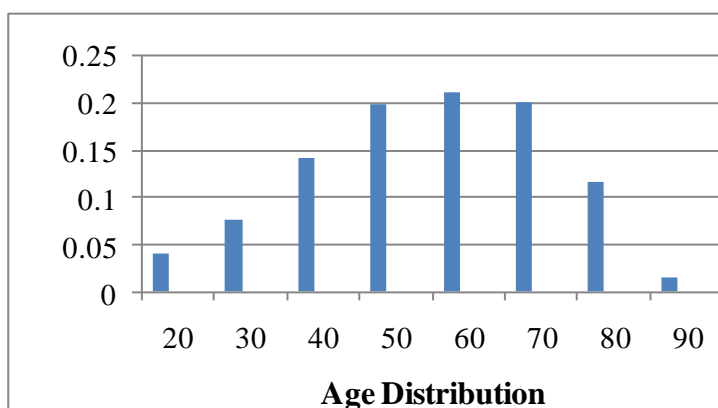


Fig 1.3 Age Distribution US (2000-2011) from the NCDB

Furthermore, anything that increases individual risk of getting a disease is called a risk factor. Having a risk factor does not mean that a patient gets cancer; not having risk factors does not mean that the patient not get cancer. Risk factors for melanoma include the following:

- Having a fair complexion which includes Fair skin that freckles and burns easily, do not tan, or tan poorly. Blue or green or other light-colored eyes. Red or blond hair.
- Being exposed to natural sunlight or artificial (such as from tanning beds) over long periods of time.
- Being exposed to certain factors in the environment. Some of the environment risk factors for melanoma are radiation, solvents, vinyl chloride, and PCBs.
- Having a history of many blistering sunburns, especially as a child or teenagers.
- Having several large or many small moles.
- Having a family history of unusual moles (a typical nevus syndrome.)
- Having a family or personal history of melanoma.

Signs of melanoma include a change in the way a mole or pigmented area looks. These and other signs and symptoms caused by melanoma or by other conditions as a mole that change in size, shape, or color which has irregular edges or borders and is more than one color. Mole is asymmetrical if the mole is divided in half; the two halves are different in size or shape. Itches, Oozes , bleeds, or is ulcerated (a hole forms in the skin when the top layer of cells breaks down and the tissue shows a change in pigmented(colored) skin. The figure 1.4 shows the signs and symptoms of malignant melanoma.

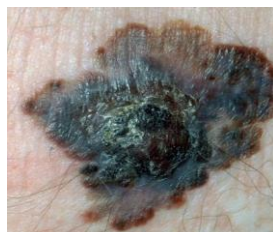


Fig 1.4: Malignant melanoma RGB color image

A. Initial research work carried out on melanoma

Although melanoma is not a new disease, evidence for its occurrence in ancient past is rather scarce. One example lies in a 1960s examination of nine peruvian Inca mummies, radiocarbon dated to be approximately 2400 years old that

showed apparent signs of melanoma that is melanotic masses in skin and diffuse metastases to the bones. John Hunter first discovered melanoma in 1787. He discovered the tumour as a “cancerous fungus” and put it in Hunterian museum in Royal College of Surgeons in England. Until 1968, tumour wasn’t tested and found to be metastasized melanoma. Melanoma was first recognized as an actual disease by Rene laenne. The first formal acknowledgement of melanoma was found untreatable is recognized by Samuel Cooper in 1840. Henry Lancaster made the connection between sunlight intensity and the development of melanoma in 1956.



John Hunter

Rene Laennec

Samuel Cooper

Henry Lancaster

Fig 1.5 Research Scientists

B. Clinical diagnosis

Clinical technicians, oncologist or dermatologist may use microscopic or photographic tools to help them visualize a lesion, in suspecting the lesion to be a skin cancer and suggest further diagnosis or a biopsy for treatment; a biopsy is a procedure where a sample of the lesion is taken for examination in the laboratory. The choice of biopsy is dependent on the size and location of the lesion, among other factors, with an excisional biopsy typically performed if the lesion is a suspected melanoma. The other types of cancer, testing of skin cancer also indicates the stage of the cancer, Staging describes widespread disease and provides physicians with information to guide treatment decisions. The American Joint Commission on cancer recommends the TNM staging system for skin cancer. T score from zero to four based on the thickness of the tumour, N score from zero to three based on how nearby lymph nodes are affected and M score based on metastasis (spread) to other parts of the body, M0 is no metastases, M1a M1b and Mc indicate varying degrees of metastasis.

C. Stages of melanoma

Suspect skin lesion melanoma are diagnosed, tests are carried out to find whether the cancer cells have spread within the skin or to other parts of the human body. Cancer spreads in three ways to the body; the method used to stage melanoma is based mainly on the thickness of the tumour and whether cancer has spread to lymph nodes or other parts of the body. The following stages are used for melanoma:

- 1) *Stage 0 (melanoma in situ)*: In stage 0, abnormal melanocytes are found in the epidermis. These abnormal melanocytes may become cancer and spread into nearby normal tissue. Stage 0 is called melanoma in situ.
- 2) *Stage I melanoma*: In stage IA, the tumour is not more than 1 millimetre thick, with no ulceration (break in the skin). In stage IB, the tumour is either not more than 1 millimetre thick, with ulceration, OR more than one but not more than two millimetres thick, with no ulceration. Skin thickness is different on different parts of the body. In stage I, cancer has formed. Stage I is divided into stage IA and IB. In stage IA, the tumour is not more than 1 millimetre thick, with no ulceration. In stage IB, the tumour is either not more than 1 millimetre thick and it has ulceration or more than one but more than two millimetre thick, with no ulceration.
- 3) *Stage II melanoma*: In stage IIA, the tumour is either more than one but not more than two millimetres thick, with ulceration (break in the skin), OR it is more than two but not more than four millimetres thick, with no ulceration. In stage IIB, the tumour is either more than two but more than four millimetres thick, with ulceration, OR it is more than four millimetres thick, with no ulceration. In stage IIC, the tumour is more than four millimetres thick, with ulceration. Skin thickness is different on different parts of the body. Stage II is divided into stage IIA, IIB and IIC. In stage IIA, the tumour is either more than one but not more than two millimetres thick, with ulceration: or more than two but not more than four millimetres thick, with no ulceration. In stage IIB, the tumour is either more than two but or more than four millimetres thick, with ulceration; or more than four millimetres thick, with no ulceration. In stage IIC, the tumour is more than four millimetres thick, with ulceration.
- 4) *Stage III melanoma*: The tumour may be any thickness, with or without ulceration (a break in the skin) and cancer has spread to one or more lymph nodes; lymph nodes with cancer maybe joined together (matted); cancer may be in a lymph vessel between the primary tumour and nearby lymph nodes; and /or very small tumours may be found on or under the skin, not more than two centimetres away from the primary tumour.
- 5) *Stage IV melanoma*: In stage IV, the cancer has spread to other places in the body, such as the lung, liver, brain, bone, soft tissue, or gastrointestinal (GI) tract. Cancer may have spread to places in the skin for away from where it first started.

D. Prevention approaches to Positive Melanoma

Despite warning against overexposure to the sun, it remains important to get a little sun exposure as this enables our bodies to produce vitamin D, an important nutrient for the prevention of diseases such as rickets and osteomalacia, As

such, sensible sun exposure is advised. Avoiding excessive exposure to ultraviolet radiation can reduce the skin cancer. This can be achieved by avoiding sunburn. Wearing clothes that protect against the summer sun that is by avoiding the highest sun intensity between 11AM and 3PM. Outdoor workers need to take particular skin care also protecting children by trying to keep them in the shade and using sun light high intensity resisting cloths, and by applying SPF 50+ sunscreen keeping babies out of direct sunlight.

The oncologist or the dermatologists recommend that tanning booths, lamps, and sun beds are not to be used. Several studies have found that caffeine intake is negatively correlated with the incidence of melanoma, with the effect of caffeine appearing to be strongest in women who consume at least 393mg of caffeine a day, it equates to around four cups of coffee.

Melanoma is a malignant disease of the skin, also called as Coetaneous Melanoma or Malignant melanoma according to the definition of the American Cancer Society (ACS) and the National Cancer Institute (NCI). Melanoma is a severe type of skin cancer, which affects the skin pigment cells called Melanocytes. The most dangerous characteristic of melanoma is that it can spread to overall body through lymphatic vessels and blood vessels. According to World Health Organization more than 65,000 people a year worldwide die due to melanoma. In Europe about 26,100 males and 33,300 females have melanoma diseases every year. The early detection of melanoma aids to increase survival rates but there is no cure for last stage of melanoma.

During the last two decades studies have observed an amazing development of imaging techniques targeted for biomedical applications. New technologies, devices and equipment combined with sophisticated analysis, visualization and storage algorithms as well as programs designed for acquisition of data, signal processing, database building or data manipulation are now available commercially. Malignant disease is one of most serious disease which causes cancer in most of the developing and under developing countries especially among woman, elderly people and young children. This research work is trying to emphasise that this disease can be prevented from serious cancer by providing proper treatments if the disease is manage to detect earliest possible.

There are worldwide efforts towards classification and recognition, prevention and diagnosis for melanoma but melanoma continues to rise at alarming state. Several attempts are made by using Image processing, artificial intelligence, neural networks, and prognosis model but even though they have considerable result we proposed better evaluation by applying decision support diagnosis system with hybridized technique by using hospitalized samples. Further, this research work focuses to construct an automated, Vision-based system for classification of Malignant Melanoma using solely the visual texture information of the lesion. The system will be based on methodologies that emanate and/or correlated with human vision therefore will closely emulate human experts only with greater extent of accuracy, reliability and reproducibility. The objective of this research work is to develop an automated melanoma skin cancer detection system with the application of ABCD rule. It includes:

Malignant melanoma is one of the very interesting topics in medical and computer science research. Incorporating the use of digital image processing techniques and ABCD rule of the said syndrome, to automatically detect the malaria disease just from the skin lesion images obtain from dermoscope can tremendously increase the speed to recognize the skin cancer by saving the time and labor cost. Use of several algorithms and libraries, to present a system that can perform a robust, real time and automated detection of malignant melanoma easily. It can help researchers to achieve approach step in order to obtain advances knowledge in this melanoma skin cancer research.

II. LITERATURE REVIEW

A. Introduction

Number of studies on the possibility of detecting malignant melanoma using various methods and techniques in the past are consider for the reviewing process. The review includes detection of melanoma using image processing concepts. The reviews are based on shape, color and size features. In previous research works the SVM and ANN is used as classifier to extract texture and geometry features of image and reviewed. In this section number of these studies is critically reviewed.

Mataz Abroras, Hani Amasha, Issa Ibraheem [1], proposed a technique for Early detection of melanoma using multispectral imaging and artificial intelligence techniques. The work describes the design of a multispectral imaging system that utilizes Artificial neural Networks and Genetic Algorithm (Artificial Intelligence) for spectral images classification. The automated diagnostic of malignant melanoma increases the cost effectiveness for treatment, reduces the detection time for illness, and reduces patient psychiatric stress caused by biopsy sampling. Wavelength scanning using filters wheel is good acquisition method as long as the region of interest does not move, otherwise captured images are addles. The result of sensitivity and specificity (for melanoma detection) is very good (>91%). Use of GA in building and training the neural network enhances performance of ANN in comparison with previous studies.

Ilias Maglogiannisa Dimitrios I. Kosmopoulosb [3] developed the Computational vision systems for the detection of malignant melanoma. In this paper, it reviews the systems by firstly presenting the visual features, then digital images processing method and artificial intelligence methods and heuristics. Authors finally compares these techniques in discriminating mailignant melanoma tumors versus Displastic naevi lesions. It uses ABCD rule of dermoscopy, pattern Analysis, Menzies method and 7-point checklist. The average success rates were 85% with the chromaticity coordinates to over pass in performance the remaining color spaces. The same team used neural networks to identify variegated coloring in skin tumors with 89% correct results. The results from both computer based system and traditional methods are compared in which mean absolute difference was about 5%. In image acquisition techniques the problem of repeatability of the measurements for follow up studies has not been satisfactorily resolved.

Jamilu Awwalu, Ali Garba Garba, Anahita Ghazvini, and Rose Atuah [4], follow Artificial Intelligence in Personalized Medicine Application of AI Algorithms in solving Personalized Medicine Problems. Here the application and ability of artificial neural network (ANN), support vector machines (SVM), Naïve Bayes, and fuzzy logic used in solving personalized medicine problems, and shows that the Obtained results meet expectations. A Successful implementation of personalized medicine would save many lived and perfect the medical profession. The implementation of personalized medicine heavily relies on AI Algorithms but it is still in its early stage and levels face and faces more challenges some of which discussed in this paper.

Omar Abuzagheh, Miad Faezipourand Buket D. Barkana [5] demonstrates Skincure: an innovative smart phone based Application to assist in melanoma early Detection and prevention. The purpose of this work is an innovative and fully functional smart-phone based application which has two major components; i.e. a real-time alert to help users prevent skin burn caused by sunlight and an automated image module analysis system which includes image acquisition, hair detection and exclusion, lesion segmentation, feature extraction, and classification. In this paper a novel equation to compute the time- to-skin-burn is introduced. The experimental results show that the proposed system is efficient, achieving classification of the normal, atypical and melanoma images with accuracy of 96.3%, 95.7% and 97.5% , respectively.

S N Deepa and B Aruna Devi [6], developed a survey on artificial intelligence approaches for medical image classification. In this work it gathers representative works that exhibit how AI is applied to the solution of very different problems related to different diagnostic science analysis. It also detects the methods of artificial intelligence that are used frequently together to solve the special problems of medicine. Artificial Intelligence, Neural Networks, Fuzzy Logic, Genetic Algorithms, Particle Swarm Optimization techniques are used. Experimental results on a set of nearly 150 cases show the proposed system to work well accurately classifying about 80%.

Maciej Ogorzalek, Leszek Nowak, Grzegorz Surowka and ana Alekseenko [8], proposed Modern techniques for computer aided melanoma diagnosis, in this work some of the standard methods of image processing for melanoma diagnosis and also new identification methods based on color decompositions are introduced. Here Image acquisition, image processing and for the Dermoscopic classification algorithms such as Artificial Neural Networks and support vector machines are used. The results confirm that neighborhood properties of pixels in Dermoscopy images record the melanoma progression and together with the selected machine learning methods may be important diagnostic aids. Especially the inductive learning approach shows great classification potential.

Arthur Tenenhaus [9], proposed a technique for Detection of melanoma from dermoscopic images of naevi acquired under uncontrolled conditions. The objective of this work is to investigate to what extent the automatic melanoma diagnosis may be achieved from the analysis of uncontrolled images of pigmented skin lesions. Here Image processing, ABCD rule, segmentation and classification methods are used. The KL-PLS based classifier shows comparable performances with respect to dermatologists (sensitivity: 95% and specificity:60%). But in this paper inclusion of other descriptors are required to increase the performance and also very small number of tumors are analyzed here.

A.Abu-Hanna, P.J.F.Lucas [10], presents Prognostic Models in Medicine. The development of prognostic models for the delivery of improved medical care is the theme of the papers included in this special issue of methods of information. It involves Statistics, Machine learning and AI. This paper illustrates ideas from AI and statistics in the context of solving the medical problem of prognosis. The method works by building and increasingly homogeneous set, in terms of the outcome, of cases that match the case at hand.

Mehi T, Binder M, Scheibboeck C, Holub S, Thomas Mehl [11], presents Integration of clinical decision support into a hospital information system to predict metastatic events in patients with melanoma. This paper supports computer-aided interpretation of pretest probability and tumor markers in patients with melanoma. In this work Arden Syntax server (CDSS), i.s.h.med (HIS) and integration techniques are used. The designated target of the dermatological project is the implementation of the joint results (pretest probability and tumor markers) as a CDSS into the HIS with a preceding reliability study of the system. According to medical view, a risk assessment of CDSS could offer substantial benefit for patients and physicians but still the final decision will be up to the physician's discretion.

Catarina Barata Jrge S. Marques Jorge Rozeira [12], proposed a technique for detecting the pigment network in dermoscopy images a directional approach. This paper reviews an algorithm for the detection network which is based on a bank of directional filters (difference of Gaussians) and explores color, directionality and topological properties of the network. It involves Pre-processing, network enhancement and network detection methods. In this paper simpler approach is used i.e compare the network area with a threshold and applies this test to divide the image into with and without pigment network classes. Experimental result shows that the algorithm achieves good detection scores. The algorithm obtained a specificity SP=67.5% and a sensibility SE=80.0%

Harald Ganster Axel Pinz Reinhard Rohrer, Ernst wilding, Michael Binder, and Harald Kittler [13], proposed a system for Automated Melanoma Recognition. A system for the computerized analysis of images obtained from ELM has been developed to enhance the early recognition of malignant melanoma. Here imaging process, segmentation feature calculation feature selection and classification methods are used. The achieved performance is about 96% of correctly segmented skin lesion images. It is possible by fusion of several simple segmentation algorithms like thresholding , color clustering etc.

I. Maglogiannis, S. Pavlopoulos, D. Koutsouris [14] proposed an Integrated Computer Supported Acquisition, Handling and Characterization System for Pigmented Skin Lesions in Dermatological Images. The paper work describes the implementation of an integrated prototype for a computer based image analysis system, intended for the characterization of dermatological images and particularly for the recognition of malignant melanoma versus dysplastic

nevus. In this paper different methods are drawn from Statistical method of discriminate analysis and artificial neural networks to find the best classification rules and to compare the results of different approaches to the problem. The results of research are even slightly better proving the significance of the standardization and reproducibility in image acquisition ensured by the proposed system.

Zhenghao Shil, and Lifeng [15], author proposed an application of neural networks in medical image processing. investigator try to answer what the major strengths and weakness of applying neural networks for medical image processing would be Image processing with neural networks, image segmentation and object detection and recognition experiments show that the neural network ensemble can achieve not only a high rate of overall identification but also a low rate of false negative identification. Artificial neural networks have some disadvantage such that a neural network is unable to express human expert's knowledge and experience with theoretical aspects and also the generalization ability will be lower if the amount of input data is less.

Paulo J. Lisboa, Azzam F. G. Taktak [16], demonstrates the use of artificial neural networks in decision support in cancer: A systematic approach. The paper reviews the clinical fields where neural network methods figure most prominently, the main algorithms featured, methodologies for model selection and the need for rigorous evaluation of results. The authors work involves Artificial neural network, statistical method and rule extraction algorithms. A review of PubMed listed publications involving clinical trials of neural network systems identified trends in areas of clinical promise, specifically in the diagnosis, prognosis and therapeutic guidance for cancer, but also the need for more extensive application of rigorous methodologies.

Wan Hussain Wan Ishak, Fadzilah Siraj [17] presents Artificial intelligence in medical application: an exploration. This paper explores the potential of artificial intelligence techniques particularly for web-based medical applications. The main characteristic of using artificial intelligence techniques in medical diagnosis and prediction is to make consultation to be more attractive. Centralized databases over the www have more advantages like information sharing, online discussion, online treatment and diagnosis and so on. Data mining, neural network and fuzzy logic are used to demonstrate the web based medical application. Further in the prediction tasks, Neural Networks have been proven to produce better results compared to other techniques (such as Statistics).

Rajesh Shankarapillai [18], developed periodontal disease risk assessment using artificial neural networks. The purpose of this work is at developing a custom neural network to predict periodontal disease risk by modifying the standard functions presently being used for multiple layer perceptron method of neural network design. The testing phase produces immediate convergence with expected accuracy and minimizes in maximum error to reach the observed parameters with reduced amount of time. This paper incorporates more periodontal risk parameters such as pan chewing, debris index, calculus index, diet and family history of periodontitis. However there is no better geographically specific mathematical custom solution that could accurately interpret the collected data to obtain more specific periodontal risk evaluation concerning subjects in pan chewing area with lower economic.

A N Ramesh, C Kambhampati, JRT Monson, PJ Drew [19], used Artificial intelligence techniques in medicine. Artificial intelligence is a branch of computer science capable of analyzing complex medical data. Their potential to exploit meaningful relationship with in a data set can be used in the diagnosis, treatment and predicting outcome in many clinical scenarios. Fuzzy expert system evolutionary computation and hybrid intelligent systems methods are used here. The proficiency of artificial intelligent techniques has been explored in almost every field of medicine. Artificial neural network was the most commonly used analytical tool.

Konstantin korotkov [20], developed a technique for Automatic change detection in multiple pigmented skin lesions, it summarizes various approaches for implementing PSL computer aided diagnosis system and discuss their standard workflow components. It uses methods such as ABCD criteria and Glasgow 7-point check list. The experimental results of algorithms for the automatic PSL, change detection in images acquired using the total body skin scanner. The result contains all necessary references to the description of algorithm.

Ammara Masood and Adel Ali Al-Jumaily [27], proposed a Computer Aided Diagnostic Support System for Skin Cancer: A review of Techniques and Algorithms. The research work aims to reposts statistics and results from the most important implementations reported to date. It compares the performance of several classifiers specifically developed for skin lesion diagnosis and discussed the corresponding findings. Image Acquisition, Pre-processing, Segmentation, Feature Extraction, Feature Selection and Classification methods are used. The results of an experimental assessment of the different designs can be the basis for choosing one of the classifiers as a final solution to the problem. In this research article the proposed system gives an important knowledge which help researchers to judge the proper feature selection method, proposed a framework for developing bench marks and standard approaches for model validation.

In the research paper written – S. Raviraja et. al. [28..30], the researchers explained the usage of image processing and statistical based approach to automatically identify and detect the number of malarial parasites per number of red blood cells and managed to do it by using color, shape and size information. In this approach the researchers proposed a method to automatically separate the parasites (trophozoites, schizonts and gametocytes) from an infected blood image using colour, shape and size information and compare the image with infected images after transformation of image by shaping and scaling to reproduce the image. The image obtained after the process of shaping and scaling, the image are then statistically analysed and compared to generate a mathematical base. The invariants moments is used to detect the nuclei of the parasites, according to a connectivity of a disk shaped structuring element where the radius is the greatest size of the red blood cells. Further evaluation of the size and shape of the nuclei of the parasite is also considered. The research work considers, total of 95 patient's clinical data plasmodium parasite infected blood smears have been diagnosed by new hybridized model. the proposed model were able to predict the parasite infected malaria disease with an accuracy of

60-96% based on selected dependent variables, validated using ROC characteristics that is, the test value of the ROC of 0.8166 and train value of ROC is 0.8209. ROC can range between 0 and 1 with higher values indicating better performance. Diagnostic models were developed to predict the parasite infected digital images. Authors suggest that the proposed application could be useful in determining potential treatment methods and monitoring the progress of treatment for infected patients.

III. DATA ANALYSIS

A. Data collection

Skin is one of the essential and largest organs in the human body. The skin pigments promote cells called Melanocytes. Melanocytes occur in the epidermis, which is the outer layer of the skin. Due to the exposure of the skin to ultraviolet rays, Skin cancer starts at the outer layer of epidermis.

Generally in skin analysis, doctors seek two kinds of skin cancers that are melanoma and non-melanoma. Melanoma is the type of skin cancer which can also be called as malignant melanoma or coetaneous melanoma. Melanoma is very dangerous and affects the skin pigment cells called Melanocytes. Melanoma is more severe than other skin cancer, because it spreads to other parts of the body but it is curable, detected early. The American Cancer Society estimates that at present, more than 135,000 new cases of melanoma in the US are diagnosed in a year. In 2015, an estimated 73,870 of these will be invasive melanomas, with about 42,670 in males and 31,200 in women. Melanoma can be identified through the discussions with the professional dermatologist, doctors and literature studies when there is change in moles. The moles grow in irregular sizes and shapes greater than 6mm diameter. Melanoma will be black or brown in color. Small amount of melanoma will be pink, red or fleshy in color. Melanoma is harder to treat when it reaches an advanced stage and spreads to other parts of the body through lymph nodes. The figure 3.1 shows the example of malignant melanoma.

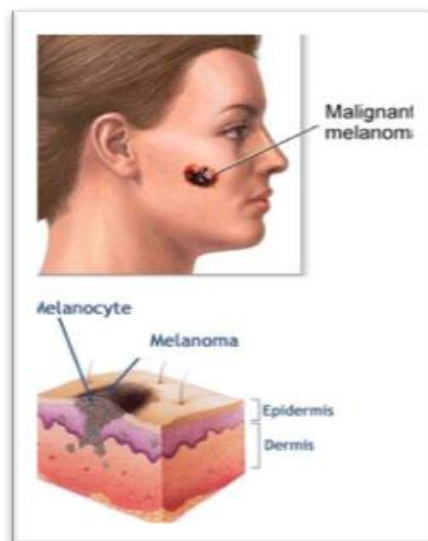


Figure 3.1 Indication of Malignant Melanoma

B. Identification of melanoma: Malignant

The national cancer institute has outlined the following characteristics for the detection of skin cancer that are associated with a higher risk of malignant melanoma:

- a. **Color** - Mixture of tan, brown, black and red/pink.
- b. **Shape** – Irregular borders which contain notches and may fade around skin with a flat portion level in the skin.
- c. **Surface** – smooth, little scaly, rough pebbly appearance.
- d. **Size** – greater than 6mm and sometimes larger than 10mm.

Melanoma can be easily identified with following symptoms.

- **A**-Asymmetrical,
- **B**-Border,
- **C**-Color Variation,
- **D**-Diameter

C. ABCD rule of dermoscopy

A melanoma can be identified using the ABCD rule of dermoscopy, which is a diagnostic algorithm used by dermatologists when analyzing dermoscopy images. This rule classifies melanocytic lesion, into a mole or a melanoma, according to its asymmetry (A), border (B), color (C) and differential dermatoscopic structures (D). The figure 3.2. [24] shows the ABCD rule for melanoma.

- **Asymmetry:** The dermoscopic image is divided by two perpendicular axes positioned to produce the lowest possible asymmetry score. If the image shows asymmetric properties with respect to both axes with regard to colours and differential structures, then the asymmetry exist.

- **Border:** In case of melanoma the lesion borders are irregular, ragged, and blurred. Therefore border are first identified and then extracted from the image leaving the inside and outside parts of the mole.
- **Color Variation:** One early sign of melanoma is the emergence of color variations in color. Because melanoma cells grow in grower pigment, they are often colorful around brown, or black, depending on the production of the melanin in the skin. The considered colors are: white, red, light-brown, dark-brown, blue-gray and black. The descriptors of color are mainly statistical parameters calculated from different color channels, like average value and standard deviation of the RGB or HSV color channel.
- **Diameter:** Melanoma tends to grow larger than common moles, and especially the diameter of 6mm. Because the wound is often irregular forms, to find the diameter, draw from all the edge pixels to the pixel edges through the midpoint and averaged. These differential structures might be: pigment network, structure less or homogeneous areas, streaks, dots and globules.

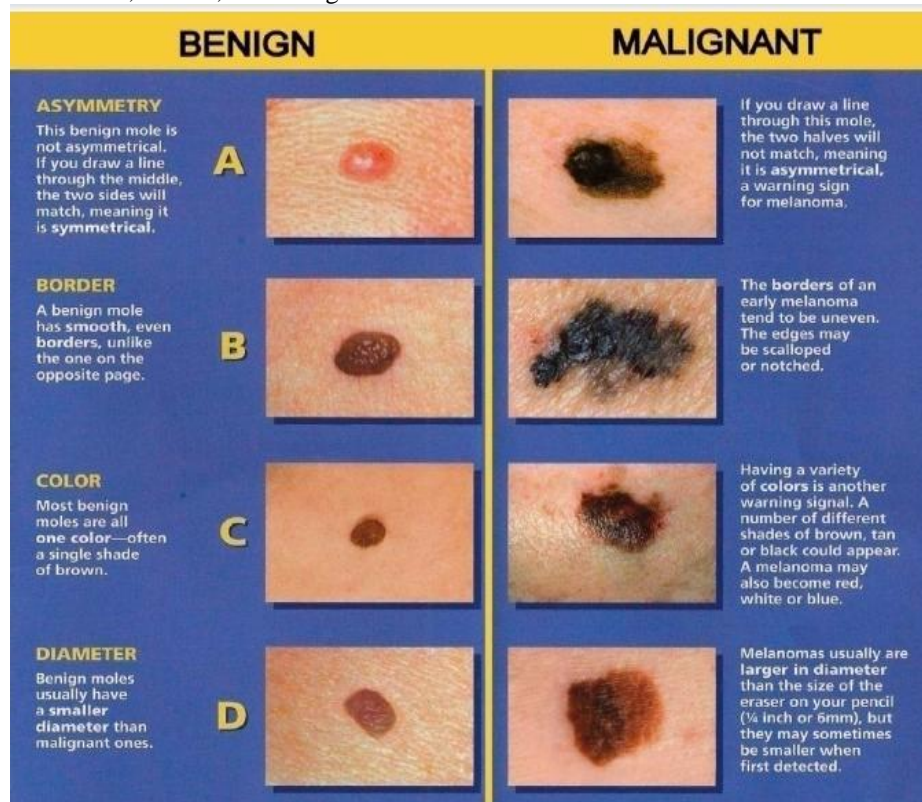


Fig 3.2 ABCD rule of dermoscopy

D. Classification of malignant melanoma

There are four main types of malignant melanoma which differ greatly in their representation as represented in figure 3.3 and Table 3.3. Those are superficial spreading malignant melanoma, Lentigo maligna melanoma, Acrallentiginous melanoma, Nodular melanoma which increases the difficulty of diagnosis.

Table 3.3: Types of malignant melanoma

Melanoma Types	Found	Remarks
Superficial Spreading	70%, neck, legs, pelvis	Considered for study
Nodular	15%, dome-shaped nodule	Considered for study
Acral-Lentiginous	8 %, Common in dark-skin	Considered for study
Lentigo Maligna	5 %, sun-exposed area, mistaken for age spot	Considered for study
Amelanotic	0.3%, non-pigmented	Not Considered for study
Desmoplastic	1.7%, ½ amelanotic	Not Considered for study

Superficial spreading melanoma is one of the common types of melanoma and 70% of melanoma is of this type. It occurs on the basal layer of epidermis. This type of melanoma appears only during the middle age, but nowadays it has increased in young adults.

Lentigo maligna melanoma is same as superficial spreading melanoma and starts from the deeper layer of skin dermis. It appears on the face, head or neck and especially on the nose and cheeks (that is mainly in areas exposed to the sun).

Acrallentiginous type of melanoma is one of the most serious types of skin cancer that arises on skin pigments. It is common in dark skinned people than fair skinned ones.

Nodular melanoma is one of the most aggressive types of melanoma. Nodular melanoma is common in elderly people. EFG (E – Elevated, F – Firm to touch, G – Growing progressively over more than a month) is a way to identify nodular melanoma easily.



Fig 3.3.1 type-1:
Superficial spreading
melanoma



Fig 3.3.2 type-2:
Lentigo maligna
melanoma



Fig 3.3.3 type-3
Acrallentiginous
melanoma



Fig 3.3.4 type-4:
Nodular melanoma

Melanomas have features indicating their melanocytic origin.

- Network
- Aggregated brown or black globules
- Site-specific features e.g. parallel pattern on palms and soles, follicular openings on facial skin
- Many other features have been described in melanoma. And they may be relatively featureless.

E. Features of superficial melanoma:

Superficial spreading melanomas typically involve intermittently sun-exposed anatomical sites such as the trunk, back and extremities. SSM usually presents as a flat slowly growing irregular lesion with variegated pigmentation that enlarges in a radial manner unless dermal invasion supervenes; this is usually signified clinically by the presence of a raised area. Superficial spreading melanoma (SSM) is recognised as a changing or distinctive lesion by the patient or their doctor, it is often large (>6mm). Characteristically, superficial melanoma is asymmetrical and irregular in shape and structure.

Superficial melanomas usually have one or more of the following dermoscopic features:

- Blue-white veil
- Multiple brown dots
- Pseudo pods
- Radial streaming
- Scar-like depigmentation
- Peripheral black dots/globules
- Multiple (5-6) colours, especially red and blue
- Broad network
- Focal sharply cut-off border
- Negative network
- Irregular vascularity

The blue-white veil is described as an irregular structure less area of confluent blue pigment with a ground glass haze, as if the image were out of focus. It is due to hyperkeratinisation over dense epidermal pigment. Uniform blue-white structures may be observed over some blue naevi and haemangiomas but in melanoma they are focal, asymmetrical and irregular.

Scar-like depigmentation due to regression of melanoma results in irregular white areas that must be distinguished from the uniform peripheral loss of pigment seen in benign halo naevi. It arises in about 50% of melanomas.

Negative network, although a feature of melanoma, may also be found in some benign melanocytic lesions (especially Spitznaevus) and seborrhoeic keratoses.

F. Features of Lentiginous melanoma

Lentiginous melanoma arises on the trunk and proximal limbs. It is usually diagnosed in the in-situ phase, and most often affects middle-aged and elderly men that have frequently exposed their backs to the sun. There is some argument regarding this entity and whether it can be distinguished from non-malignant atypical junctional hyperplasia or atypical junctional naevus in the elderly. Dermoscopy may show features of solar lentigo, melanoma in situ and/or superficial spreading melanoma.

- Irregular shape, structure and colour
- Grey or brown lines forming polygons (larger than perifollicular rhomboid structures of lentigo maligna)
- Grey dots
- Multiple hypopigmented areas
- Structure less areas
- Fine pigment network or fingerprinting

G. Features of Nodular melanoma

Clinically Nodular melanomas may be confused with other cutaneous tumours such as basal cell carcinomas, particularly if they are amelanotic. Histologically in NM, there is no epidermal component extending beyond the edges of the dermal component (a "cut off" of three rete ridges is used by some authors). It can also be missed by dermoscopy if

melanoma features are not noted on the periphery of the lesion. The lesion may composed of only two or three colours and these may be distributed fairly symmetrically. Sixty percent of nodular melanoma is amelanotic. Features often include:

- Isolated globules
- Blue-grey veil
- White streaks
- Irregular linear or dotted vessels

Nodular lesions with suspicious features should be excised rather than followed up – delay may be dangerous. They may resemble seborrheic keratosis, basal cell carcinoma or angioma.

H. Features of Acral melanoma

Acral melanoma (palms and soles) tends to be much deeper than is suspected from its flat nature. Dermoscopically, it is characterised by a broad parallel ridge pattern rather than the benign parallel furrow pattern. The asymmetry and other features of superficial melanoma may be present.

Little white dots on the ridges are sweat ducts (acrosyringia) and confirm palmoplantar location. In melanoma, these dots disappear because the acrosyringia are destroyed by the malignant process.

Subungual melanoma is a type of acral melanoma. Early lesions may show widening pigmented bands, irregular in spacing and varying colour (including pink or red in amelanotic melanoma). A positive Hutchinson's sign refers to pigment arising on the skin to the nail, which is rare in benign naevi. Changes may be observed by dermoscopy before they are evident clinically. Single pigmented bands should be followed by dermoscopy after several months.

IV. RESEARCH METHODOLOGY

This section briefly narrates the methodology adopted in the proposed research work. The discussion starts with the problem identification, the nature data for this research, the data preparation, and followed by the discussion on the development of ABCD rule based model for recognition and classification of the melanoma.

A. Image processing Concepts

An image may be defined as a 2D function, where x and y are spatial coordinates, and the amplitude of at any pair of coordinates is called the intensity or gray level of the image at that point. When x , y and the amplitude values are all finite discrete quantities, we call the image a digital image. The field of digital image processing (DIP) refers to processing digital images by means of a digital computer/ devices. Note that a digital image is composed of a finite number of elements, each of which has a particular location and value. These elements are referred to as picture elements, image elements, and pixels. Pixel is the term most widely used to denote the elements of a digital image.

A digital image $a[m,n]$ described in a 2D discrete space is derived from an analog image $a(x,y)$ in a 2D continuous space through a sampling process that is frequently referred to as digitization. The 2D continuous image $a(x,y)$ is divided into N rows and M columns. The intersection of a row and a column is termed as a pixel. The value assigned to the integer coordinates $[m,n]$ with $\{m=0,1,2,\dots,M-1\}$ and $\{n=0,1,2,\dots,N-1\}$ is $a[m,n]$. In fact, in most cases $a(x,y)$ which we might consider to be the physical signal that impinges on the face of a 2D sensor is actually a function of many variable including depth (z), color (λ), and time (t). Unless otherwise stated, we will consider the case of 2D, monochromatic, static images in this research.

Dermoscopy is an imaging methodology for the examination of skin lesions. This method provides a good and detailed view of the lesions. The imaging equipment used for taking the images is Dermatoscope. It is a handheld device which is compact and easy to use. Dermoscopic images are basically digital Photographs or images of magnified skin lesion, taken with conventional camera equipped with special lens extension. The lens attached to the dermatoscope acts like a microscope magnifier with its own light source that illuminates the skin surface evenly. Digital images acquired using photon dermatoscope are sufficiently high resolution to allow for precise analysis in terms of differential structures appearance. Dermatologist creates accurate documentation of gathered images is shown in figure 4.1 [26], opening a path for computer analysis, where images are processed in order to extract information that can later used to classify those images.

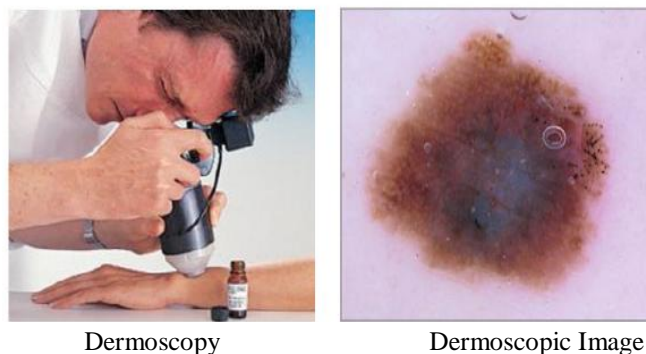


Fig 4.1 Dermoscopic Method for capturing image

Image database consisting of Original Melanoma images

- 204x200 24-bit color images digitized from 35mm color photographic slides and photographs
- 120 melanoma images
- Border images: Binary images drawn manually and reviewed by the dermatologist for accuracy

An image from dermoscopy is prone to differ widely in the foreground or the background color due to several conditions. This may be due to difference in the light source or filters, cameras, slide preparation. In order to have an analysis towards constant color characteristics, the images are normalized. In this work, the gray level normalization is incorporated through which a constant gray value of the image is maintained which does not change to different conditions. In a diagonal model, an image of unknown illumination I_u can be simply transformed to the known illuminant space I_k by multiplying pixel values with a diagonal matrix ($I_k r g b(x) = M I_u r g b(x)$). Where $\mu_l r g b$ are the mean for channels r,g,b. The constant grey values for each channels was assumed to be 255 (the maximum possible value) which is similar to colourless transparent pixel color. Further the normalized image is transformed to LAB color space. This color space is chosen because the L layer of the image has the image intensity as one of its component which ensures the contrast enhancement and equalization in more efficient way compared to other color spaces. The processed LAB color space image is converted back to RGB color space. The corrected RGB image is segmented using histogram based thresholding operation. This step ensures the removal of noise and artefacts to major extent without missing the infected lesion. Since the protocol is dominant towards other color components, the threshold is applied on the green component of the RGB image. The regional maxima and minima were used as markers and thresholded images were reconstructed in order to avoid objects that are artefacts. The objects in the above process of object detection are called for both the normalized image and the original input RGB image. The detection using normalized image outputs a binary image which ensures the reconstruction of cells that are of interest and with very minimal artefacts which tends to be appearing as cells or due to intensity factors. This image is used as marker and the object detection using original input RGB is used as the mask image. A general reconstruction is performed between the mask and the morphologically (disk of constant radius) eroded marker image. The reconstructed image is added with the marker image in order to retain the original structure of the skin lesion.

B. Image pre-processing

The general practice of any application development of the vision based systems primarily aims to make the acquired images more suitable for subsequent processes mainly image segmentation and feature extraction. There are basic three main objectives for image pre-processing: a) to re-size the image for the purposes of either magnifying the image through digital zooming, or reducing the image size in order to speed up processing. b) Image pre-processing is to reduce or eliminate noise from the acquired image and c) to enhance the image contrast for visual evaluation.

In the case of malignant melanoma digital images are captured by dermoscope, digital zooming and contrast enhancement is not necessary since the task of image classification and recognition is to be performed by a machine and not a human operator. However, image size normalization is essential in order to standardize the spatial resolution for images from different sources. Image filtering is also necessary in order to reduce or eliminate noise in images which could have been acquired during the process of sample preparation or image acquisition.

C. Feature Extraction: Color

A total of 73 samples were used for experiment. Each sample had number of normal and infected skin lesion along with artefacts. The objects extracted from these samples are melanoma. In order to classify the identified objects, the feature includes intensity based Histogram features and shape measurement features. These features are extracted for different channel of color spaces namely gray, hue, saturation and luminosity (standard deviation). First Order Statistical Features / Histogram Features: The histogram counts and the bin locations are pixel counts and bin (256) respectively. The first order features are defined by the following equations, reconstructed image are labelled.

Shape Measurement Features: Since these features are independent of color spaces, the following equations were directly applied to the binary mask image. Shape measurements can detect the changes in the size. The advantage of shape measurements is straightforward interpretation of the calculated feature values.

At this stage of selecting suitable parameters which adequately describes the information of the image and parameters are grouped together in vector form, and are referred to as feature vectors. Features can be obtained directly from images example raw image pixel values or they could be derived quantities such as average image intensity, image histogram moments, shape signature and object area.

1) HSV Color Space Transformation

HSL, HSV, HSI, or related models are often used in computer vision and image analysis for feature detection or image segmentation. The applications of such tools include object detection, for instance in robot vision; object recognition, for instance of faces, text, or license plates; content-based image retrieval; and analysis of medical images. In the most part of computer vision algorithms used on color images are straightforward extensions to algorithms designed for greyscale images, for instance k-means or fuzzy clustering of pixel colors, or canny edge detection. At the simplest, each color component is separately passed through the same algorithm. It is important, therefore, that the features of interest be able to be distinguished in the color dimensions used. Since the R, G, and B components of an object's color in a digital image are all correlated with the amount of light hitting the object, and therefore with each other, image descriptions in terms of those components make object discrimination difficult. Descriptions in terms of hue/ lightness/ chroma or hue/lightness/saturation are often more relevant.

In the beginning of late 1970s, transformations like HSV or HSI were used as a compromise between effectiveness for segmentation and computational complexity. They can be thought of as similar in approach and intent to the neural processing used by human color vision, without agreeing in particulars: if the goal is object detection, roughly separating hue, lightness, and chroma or saturation is effective, but there is no particular reason to strictly mimic human color response. The function of color map $\text{cmap} = \text{rgb2hsv}(M)$ converts an RGB colormap M to an HSV colormap cmap . Both colormaps are m -by-3 matrices. The elements of both colormaps are in the range 0 to 1.

The columns of the input matrix M represent intensities of red, green, and blue, respectively. The columns of the output matrix cmap represent hue, saturation, and value, respectively.

The function $\text{hsv_image} = \text{rgb2hsv}(\text{rgb_image})$ converts the RGB image to the equivalent HSV image. RGB is an m -by- n -by-3 image array whose three planes contain the red, green, and blue components for the image. HSV is returned as an m -by- n -by-3 image array whose three planes contain the hue, saturation, and value components for the image.

2) Binarization and Region Detection Using ROI and BW Region.

A binary image is a digital image that has only two possible values for each pixel. Typically the two colors used for a binary image are black and white though any two colors can be used. The color used for the object(s) in the image is the foreground color while the rest of the image is the background color.[1] In the document-scanning industry this is often referred to as "bi-tonal". Binary images are also called bi-level or two-level. This means that each pixel is stored as a single bit that is 0 or 1. The names B&W, monochrome or monochromatic are often used for this concept, but may also designate any images that have only one sample per pixel, such as greyscale images. In Photoshop parlance, a binary image is the same as an image in "Bitmap" mode. Binary images often arise in digital image processing as masks or as the result of certain operations such as segmentation, thresholding, and dithering. Several input/output devices, such as laser printers, fax machines, and bi-level computer displays, can only handle bi-level images.

A binary image is stored in memory as a bitmap, a packed array of bits. A 640×480 image requires 37.5 KiB of storage, and because of the small size of the image files, fax machine and document management solutions usually use this format. Most binary images also compress well with simple run-length compression schemes. Binary images can be further interpreted as subsets of the two-dimensional integer lattice Z^2 ; the field of morphological image processing was largely inspired by this view [30].

3) Gaussian Filter

Since all edge detection results are easily affected by image noise, it is essential to filter out the noise to prevent false detection caused by noise. To smooth the image, a Gaussian filter is applied to convolve with the image as shown in figure 4.3. This step will slightly smooth the image to reduce the effects of obvious noise on the edge detector. The equation for a Gaussian filter kernel with the size of $2k+1 \times 2k+1$ is shown as follows:

$$H_{ij} = \frac{1}{2\pi\sigma^2} * \exp\left(-\frac{(i-k-1)^2 + (j-k-1)^2}{2\sigma^2}\right)$$

Following is an example of a 5×5 Gaussian filter, used to create the image to the right, with $\sigma = 1.4$. (The asterisk denotes a convolution operation.)

$$B = \frac{1}{159} \begin{bmatrix} 2 & 4 & 5 & 4 & 2 \\ 4 & 9 & 12 & 9 & 4 \\ 5 & 12 & 15 & 12 & 5 \\ 4 & 9 & 12 & 9 & 4 \\ 2 & 4 & 5 & 4 & 2 \end{bmatrix} * A.$$

It is important to understand that the selection of the size of the Gaussian kernel will affect the performance of the detector. The larger the size is, the lower the detector's sensitivity to noise. Additionally, the localization error to detect the edge will slightly increase with the increase of the Gaussian filter kernel size. A 5×5 is a good size for most cases, but this will also vary depending on specific situations.

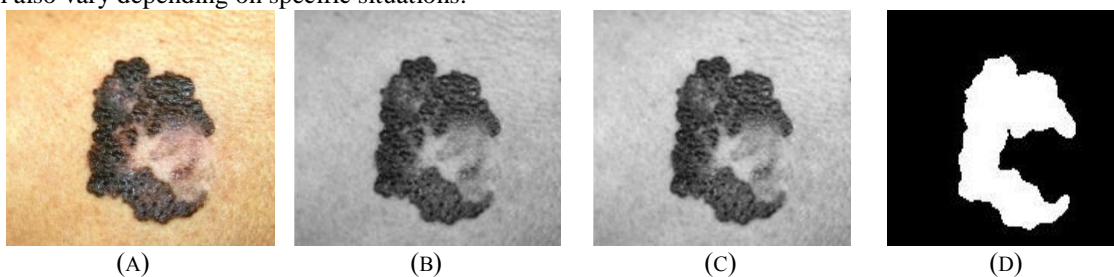


Fig 4.3: Removal of noise using 2D Gaussian filtering

(a). Original image with noise and distortion, (b). Grayscaled image, (c). Image after Gaussian Noise removal (d) Binarized image

4) Finding the Intensity Gradient of the Image

An edge in an image may point in a variety of directions, so the Canny algorithm uses four filters to detect horizontal, vertical and diagonal edges in the blurred image. The edge detection operator (Roberts, Prewitt, Sobel for example) returns a value for the first derivative in the horizontal direction (G_x) and the vertical direction (G_y). From this the edge gradient and direction can be determined:

$$G = \sqrt{G_x^2 + G_y^2}$$

$$\Theta = \text{atan2}(G_y, G_x),$$

Where G can be computed using the hypot function and atan2 is the arctangent function with two arguments. The edge direction angle is rounded to one of four angles representing vertical, horizontal and the two diagonals (0, 45, 90 and 135 degrees for example). An edge direction falling in each color region will be set to a specific angle values, for example alpha lying in yellow region (0 to 22.5 degrees and 157.5 degrees to 180 degrees) will be set to 0 degree.

Non-maximum suppression is an edge thinning technique. Non-Maximum suppression is applied to "thin" the edge. After applying gradient calculation, the edge extracted from the gradient value is still quite blurred. With respect to criteria 3, there should only be one accurate response to the edge. Thus non-maximum suppression can help to suppress all the gradient values to 0 except the local maximal, which indicates location with the sharpest change of intensity value. The algorithm for each pixel in the gradient image is:

- a) Compare the edge strength of the current pixel with the edge strength of the pixel in the positive and negative gradient directions.
- b) If the edge strength of the current pixel is the largest compared to the other pixels in the mask with the same direction (that is, the pixel that is pointing in the y direction, it will be compared to the pixel above and below it in the vertical axis), the value will be preserved. Otherwise, the value will be suppressed.

D. Feature Extraction: Normalization

1) The Histogram of Oriented Gradients and wavelet method

The histogram of oriented gradients (HOG) is a feature descriptor used in computer vision and image processing for the purpose of object detection. The technique counts occurrences of gradient orientation in localized portions of an image. This method is similar to that of edge orientation histograms, scale-invariant feature transform descriptors, and shape contexts, but differs in that it is computed on a dense grid of uniformly spaced cells and uses overlapping local contrast normalization for improved accuracy.

The essential thought behind the histogram of oriented gradients descriptor is that local object appearance and shape within an image can be described by the distribution of intensity gradients or edge directions. The image is divided into small connected regions called cells, and for the pixels within each cell, a histogram of gradient directions is compiled. The descriptor is then the concatenation of these histograms. For improved accuracy, the local histograms can be contrast-normalized by calculating a measure of the intensity across a larger region of the image, called a block, and then using this value to normalize all cells within the block. This normalization results in better invariance to changes in illumination and shadowing.

The HOG descriptor has a few key advantages over other descriptors. Since it operates on local cells, it is invariant to geometric and photometric transformations, except for object orientation. Such changes would only appear in larger spatial regions. Moreover, as Dalal and Triggs discovered, coarse spatial sampling, fine orientation sampling, and strong local photometric normalization permits the individual body movement of pedestrians to be ignored so long as they maintain a roughly upright position. The HOG descriptor is thus particularly suited for human detection in images.

The first step of calculation in many feature detectors in image pre-processing is to ensure normalized color and gamma values. As Dalal and Triggs point out, however, this step can be omitted in HOG descriptor computation, as the ensuing descriptor normalization essentially achieves the same result. Image pre-processing thus provides little impact on performance. Instead, the first step of calculation is the computation of the gradient values. The most common method is to apply the 1-D centered, point discrete derivative mask in one or both of the horizontal and vertical directions. Specifically, this method requires filtering the color or intensity data of the image with the following filter kernels:

$$[-1, 0, 1] \text{ and } [-1, 0, 1]^T.$$

Dalal and Triggs tested other, more complex masks, such as the 3x3 Sobel mask or diagonal masks, but these masks generally performed poorer in detecting humans in images. They also experimented with Gaussian smoothing before applying the derivative mask, but similarly found that omission of any smoothing performed better in practice.

2) Orientation binning

The second step of calculation is creating the cell histograms. Each pixel within the cell casts a weighted vote for an orientation-based histogram channel based on the values found in the gradient computation. The cells themselves can either be rectangular or radial in shape, and the histogram channels are evenly spread over 0 to 180 degrees or 0 to 360 degrees, depending on whether the gradient is "unsigned" or "signed". Dalal and Triggs found that unsigned gradients used in conjunction with 9 histogram channels performed best in their human detection experiments. As for the vote weight, pixel contribution can either be the gradient magnitude itself, or some function of the magnitude. In tests, the gradient magnitude itself generally produces the best results. Other options for the vote weight could include the square root or square of the gradient magnitude, or some clipped version of the magnitude.

3) Descriptor blocks

In order to account for changes in illumination and contrast, the gradient strengths must be locally normalized, which requires grouping the cells together into larger, spatially connected blocks. The HOG descriptor is then the concatenated vector of the components of the normalized cell histograms from all of the block regions. These blocks typically overlap, meaning that each cell contributes more than once to the final descriptor. Two main block geometries exist: rectangular R-HOG blocks and circular C-HOG blocks. R-HOG blocks are generally square grids, represented by three parameters: the number of cells per block, the number of pixels per cell, and the number of channels per cell histogram. In the Dalal and Triggs human detection experiment, the optimal parameters were found to be 3x3 cell blocks of 6x6 pixel cells with 9 histogram channels. Moreover, they found that some minor improvement in performance could be gained by applying a Gaussian spatial window within each block before tabulating histogram votes in order to weight pixels around the edge

of the blocks less. The R-HOG blocks appear quite similar to the scale-invariant feature transform (SIFT) descriptors; however, despite their similar formation, R-HOG blocks are computed in dense grids at some single scale without orientation alignment, whereas SIFT descriptors are usually computed at sparse, scale-invariant key image points and are rotated to align orientation. In addition, the R-HOG blocks are used in conjunction to encode spatial form information, while SIFT descriptors are used singly.

Circular HOG blocks (C-HOG) can be found in two variants: those with a single, central cell and those with an angularly divided central cell. In addition, these C-HOG blocks can be described with four parameters: the number of angular and radial bins, the radius of the center bin, and the expansion factor for the radius of additional radial bins. Dalal and Triggs found that the two main variants provided equal performance, and that two radial bins with four angular bins, a center radius of 4 pixels, and an expansion factor of 2 provided the best performance in their experimentation. Also, Gaussian weighting provided no benefit when used in conjunction with the C-HOG blocks. C-HOG blocks appear similar to shape context descriptors, but differ strongly in that C-HOG blocks contain cells with several orientation channels, while shape contexts only make use of a single edge presence count in their formulation.

4) Block normalization

Dalal and Triggs explored four different methods for block normalization. Let \mathbf{v} be the non-normalized vector containing all histograms in a given block, $\|\mathbf{v}\|_k$ be its k-norm for $k = 1, 2$ and ϵ be some small constant (the exact value, hopefully, is unimportant). Then the normalization factor can be one of the following:

$$f = \frac{v}{\sqrt{\|v\|_2^2 + \epsilon^2}}$$

L2-norm:

L2-hys: L2-norm followed by clipping (limiting the maximum values of v to 0.2) and renormalizing

$$f = \frac{v}{(\|v\|_1 + \epsilon)}$$

L1-norm:

$$f = \sqrt{\frac{v}{(\|v\|_1 + \epsilon)}}$$

L1-sqrt:

In addition, the scheme L2-hys can be computed by first taking the L2-norm, clipping the result, and then renormalizing. In their experiments, Dalal and Triggs found the L2-hys, L2-norm, and L1-sqrt schemes provide similar performance, while the L1-norm provides slightly less reliable performance; however, all four methods showed very significant improvement over the non-normalized data.

Histogram of oriented gradients (HOG) is a feature descriptor used to detect objects in computer vision and image processing. The HOG descriptor technique counts occurrences of gradient orientation in localized portions of an image - detection window, or region of interest (ROI) and are also used in [30].

Implementation of the HOG descriptor algorithm is as follows:

- Step 1: Divide the image into small connected regions called cells, and for each cell compute a histogram of gradient directions or edge orientations for the pixels within the cell.
- Step 2: Discretize each cell into angular bins according to the gradient orientation.
- Step 3: Each cell's pixel contributes weighted gradient to its corresponding angular bin.
- Step 4: Groups of adjacent cells are considered as spatial regions called blocks. The grouping of cells into a block is the basis for grouping and normalization of histograms.
- Step 5: Normalized group of histograms represents the block histogram. The set of these block histograms represents the descriptor.

The following figure demonstrates the algorithm implementation scheme:

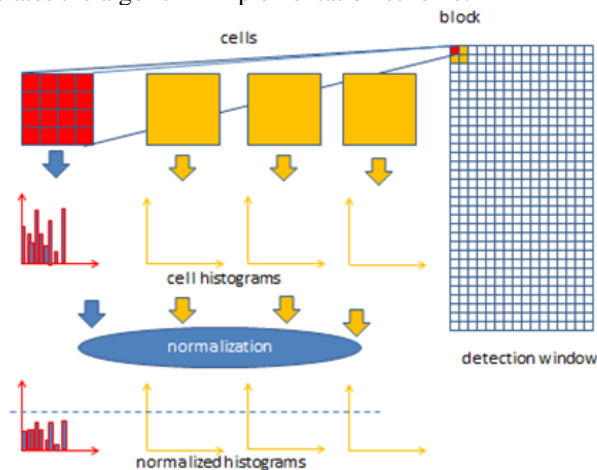


Fig 4.5: HOG descriptor algorithm

Computation of the HOG descriptor requires the following basic configuration parameters:

- Masks to compute derivatives and gradients
- Geometry of splitting an image into cells and grouping cells into a block

- Block overlapping
- Normalization parameters

According to Dalal the recommended values for the HOG parameters are:

- 1D centered derivative mask [-1, 0, +1]
- Detection window size is 64x128
- Lesion size is 8x8
- Block size is 16x16 (2x2 cells)

E. Segmentation

The segmentation stage is one of the most important since it affects the accuracy of the subsequent steps. Image segmentation is the key behind image understanding and it is the prime area of research in computer vision. However, segmentation is difficult because of the great variety of lesion shapes, sizes, and colors along with different skin types and textures. In addition, few lesions have irregular boundaries. Image segmentation involves image partitioning into multiple segments or regions of interest. Segmentation helps in grouping similar characteristics regions, and further is a process of extracting and representing information from the image to group pixels together with region of similarity.

The aim of segmentation is converting the image representation into a meaningful one for simplification in image analysis. In this process a label is assigned to each pixel, such that pixels with same labels share common visual characteristics. Image segmentation is used to locate skin lesions and their boundaries. In the proposed vision based system are using Watershed segmentation method, because of its popularity due to generation of less complex computational results.

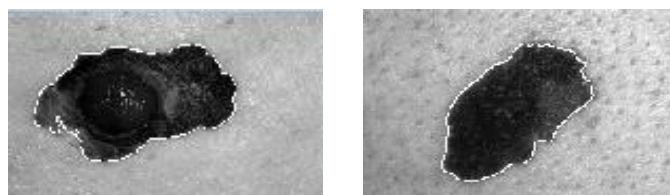


Fig 4.6 Segmentation of images

F. Feature Extraction: ABCD

In order to diagnose skin lesion automatically we will follow feature extraction process. A process is based on the rule that is ABCD rule of dermatoscopy. ABCD stands for asymmetry, colour, variation, border structure and dermatoscopical structure which is also called diameter of the lesion.

1) Asymmetry

One-half of the lesions do not match the other. Asymmetry is calculated by dividing the image over its closest line of symmetry (that is., centroid). Finding the area of the non overlapping sections and then the difference between these areas. The obtained result is divided by total area. The mathematical expression used to calculate percentage of asymmetry is:-

$$\text{Asymmetry} = (\Delta P / P) * 100$$

Where, ΔP = Pixel difference

P = Total Pixel count of lesion

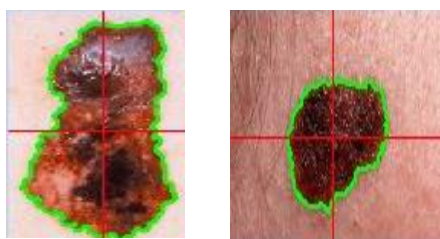


Fig 4.7 Asymmetry of images

2) Border:

In case of melanoma the borders of the lesion are irregular, ragged, notched, or blurred. So, the edge or the border are first recognized and then fetched from the image excluding the inner, outer parts of the mole[23]. To determine border irregularity, we will follow many different measures like: compactness index, fractal index, edge abruptness, pigment transition.

- i) **Compact Index** : Compact Index can be determined by using the following equation:

$$CI = (P^2 / L) = (4AL)$$

Where, PL = Perimeter of the Lesion.

AL = Area of the Lesion.

- ii) **Fractal Dimension**: The fractal dimension can be used as a characteristic of an image. Fractal dimension can be calculated by the method of calculation of the box (box-counting). To find the fractal dimension of an image, the Hausdorff dimension calculation method is simpler and effective one.

3) Color Index

Color index is calculated by converting the input image to hsv image value by checking the presence of the following colors[25][28][30]. Length of all the available pixels with given values is divided by total number of pixels. The presence of color is dependent on the value of resultant not equal to zero. For each color present the Color Index is +1.

4) Diameter

The diameter value is said to be 5 if the diameter of lesion is greater than 6mm. For other values the diameter is one less than its actual rounded value. In order to calculate Diameter the regionprops function is used to get the minor axis length of the lesion region. Resultant value is converted into mm value and the value is assigned to diameter. The flow of the entire ABCD Algorithm is depicted in a flow chart as shown in figure 4.8 [21]

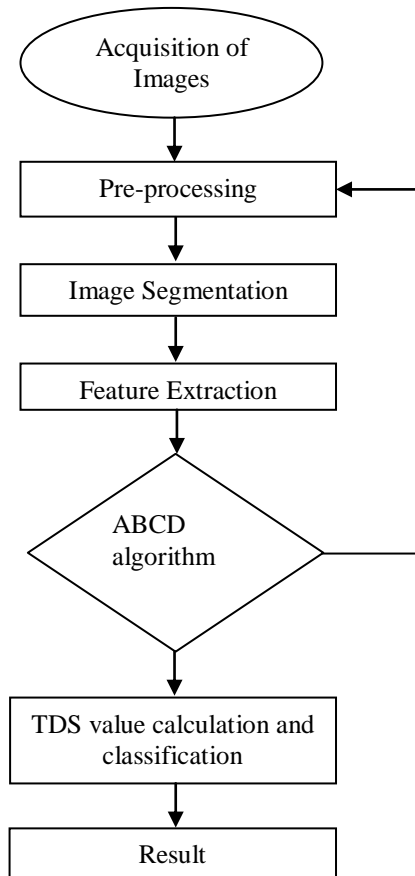


Fig 4.8 Design flow of ABCD algorithm

G. Classification

TDS score is a best solution which can be carried out by using following formula used for classification.

$$TDS = 1.3A + 0.1B + 0.5C + 0.5D$$

Actual code which is in algorithmic calculation using MatLab code is as follows;

```

Bo = CI+fractal+l+lg+VI;
Co=k+w+b+r+d+o+y+g+c+m;
Do=DIA;
%TDV=
1.3*AI+0.5*w+0.5*k+0.6*o+0.5*d+0.5*b+0.5*r+0.5*CI+0.5*l+0.5*lg+0.5*fractal+0.5*VI+0
.5*DIA;
TDV= 1.3*AI+0.1*Bo+0.5*Co+0.5*Do;
  
```

As shown in Table 4.1 [21], if the TDS Index is less than 4.75, it is benign (noncancerous) skin lesion. If TDS Index is greater than 4.75 and less than 5.45, it is suspicious case of skin lesion. If TDS Index is greater than 5.45, it is malignant melanoma (cancerous) skin lesion [25].

Table 4.1 Final classifications for ABCD rule

Total Dermoscope value (TDS)	Interpretation
<4.75	Benign or Non Melanoma
4.8-5.45	Suspicious Melanoma
>5.45	Melanoma

The proposed system components are stored or captured microscopic images from the root directory, a data entry program to create, add, and delete the image files and finally a diagnosis program which makes the matching process. The table consists of the following programming files as shown in Table 4.2

Table 4.2: Code files

Program Code	Code Description
Segmentation.m	segaml fo noitatnemgeS
Colorhistogram.m	Color extraction
Total_score.m	Classification
Melanoma.m	Application window
Melanoma.fig	Image window
Image-conversion.m	Conversion of images
Asymetry.m	Asymetry of image
Fractal_dimension.m	latcarf dinoisnem fo egami
Pigmenttranslation.m	noitatnemgip
edgeradialVar.m	Edge calculation
retemaid.m	Diameter of image

H. System Architecture

In the proposed architectural building model work as designed in Figure 4.9, the desired image capture or the selection used as an input to the proposed model. The stage 1 block of inter connected programming modules comprises the image pre processing and segmentation algorithms. The Stage 2 of the system architecture border or the edge detection, finding out the ROI of the desired pre-processed image along the algorithms for evaluating geometric information such as shape and size. Further the stage 2 concludes by calculating the TDS Scores based on the feature extraction and the ABCD rules and stage 3 for displaying the findings or the results out of stage 1 & 2.

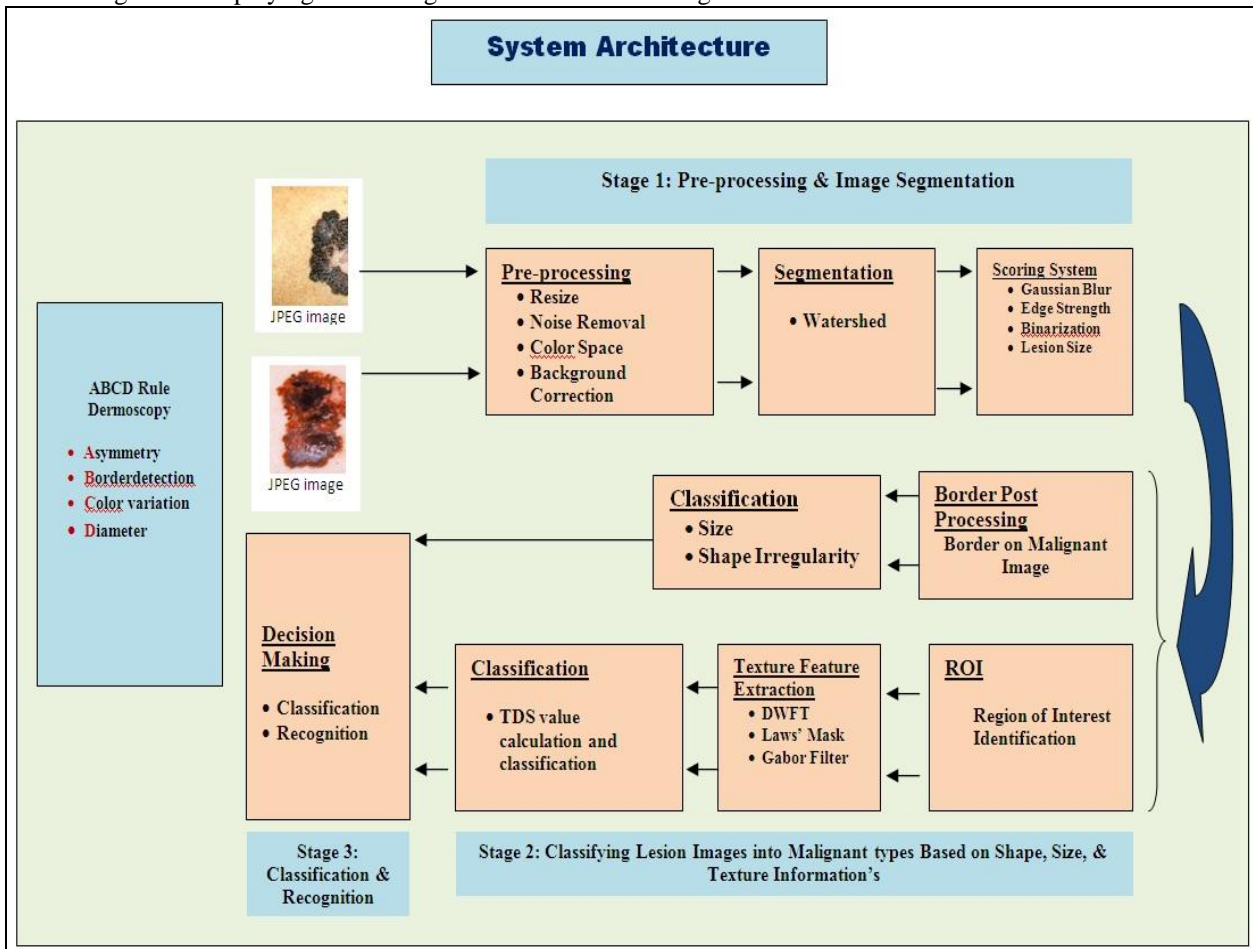


Fig 4.9 System architecture of Computational System

The procedure of ABCD algorithm is to quantitatively assess each of the four mentioned categories and assign them a numeric value. Each score is scaled by a weight factor indicating empirically determined importance, and then the sum of these weighted scores yields the total dermatoscopy score, or TDS. It is possible to concluded from the results that the proposed system is effectively used by patients and physicians to diagnose the skin cancer more accurately

V. RESULT DISCUSSION

A new experimental diagnostic model design has been developed to be used in the classification and recognition. Where other research work used moving average method for the experimental data design, in this research the data are prepared using image processing from the clinical dataset. However, using the clinical dataset, the ABCD models are successful in recognizing the Melanoma of the clinical image. The diagnosis system automatically detects the melanoma skin cancer according to the classification and recognition algorithm. The table 5.1 shows the Data samples.

Table 5.1 Skin cancer Clinical Data Samples.

Type	No. Of Samples
amonaleM	52
amonaleM noN	15
suoicipsuS	05

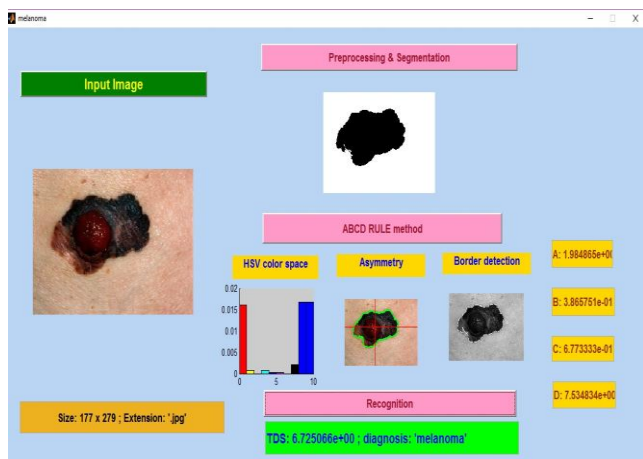


Fig 5.1 : Result of Malignant melanoma detection

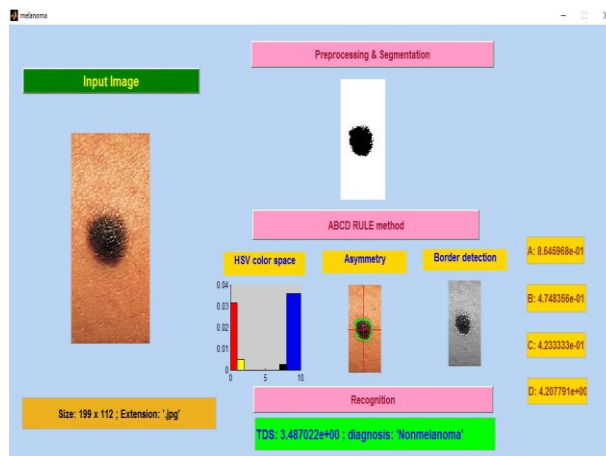


Fig 5.2: Result of Non melanoma detection

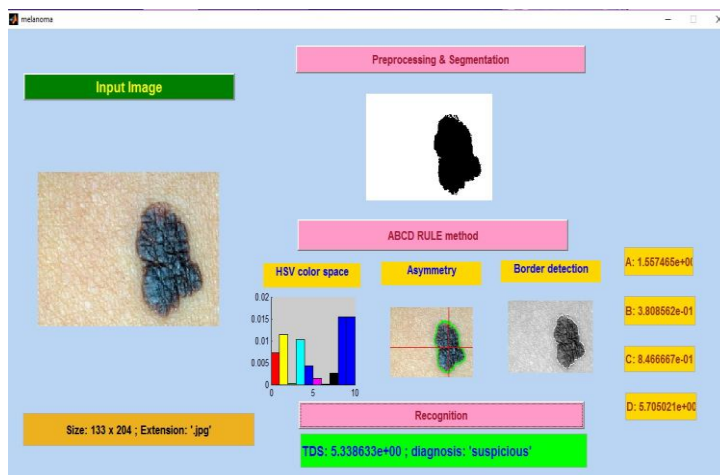


Fig 5.3 : Result of Suspicious melanoma

Table 5.2: Comparisons between investigation and system results.

Image No	A Factor	B Factor	C Factor	D Factor	TDS Score	Conclusion	Result
M1	4.5953	0.39677	0.508	11.032	11.78579	Melanoma	True
M2	1.82736	0.36879	4.2333	7.0702	6.15923	Melanoma	True
M3	2.0271	0.41142	0.84667	6.9388	6.5692	Melanoma	True
M4	1.886	0.3588	0.4233	8.237	6.8179	Melanoma	True
M5	0.8827	0.4793	0.84667	6.0704	4.654053	nonMelanoma	False
M6	0.98302	0.4207	0.762	7.252	5.3277	Suspicious	True
M7	2.8289	0.5956	0.84666	10.358	9.3394	Melanoma	True
M8	3.4535	0.38869	0.67733	7.6222	8.6783	Melanoma	True
M9	1.5575	0.38085	0.84666	5.705	5.3386	Suspicious	True
M10	4.2869	0.56129	0.84666	12.813	12.459	Melanoma	True
M11	2.3391	0.4622	0.84666	7.1905	7.1057	Melanoma	True

M12	1.9848	0.38657	0.6773	7.5384	6.72506	Melanoma	True
M13	1.73815	0.49177	0.508	6.6128	5.8691	Melanoma	True
M14	2.0995	0.47625	0.762	6.2716	6.2938	Melanoma	True
M15	1.6562	0.70213	0.762	8.2954	6.752	Melanoma	True
M16	1.20053	0.55097	0.338666	6.06748	4.8188	Suspicious	True
M17	1.1453	0.3858	0.42333	5.9129	4.69554	NonMelanoma	False
M18	0.8989	0.4014	0.67733	4.4821	3.78843	nonMelanoma	False
M19	1.4089	0.4659	0.42333	6.7664	5.47297	Melanoma	True
M20	1.53841	0.3298	0.42333	7.4611	5.97511	Melanoma	True
M21	2.831179	0.33501	0.508	10.2734	9.1047	Melanoma	True
M22	0.7497	0.2765	0.762	5.1852	3.975867	NonMelanoma	False
M23	2.23691	0.55586	0.592667	7.3849	6.958237	Melanoma	True
M24	3.964268	0.4408	0.84666	10.5609	10.90145	Melanoma	True
M25	2.19767	0.6937	0.84667	9.61984	8.15961	Melanoma	True
M26	5.05581	0.4465	0.67733	13.17898	13.5453	Melanoma	True
M27	1.68111	0.37947	0.762	5.3263	5.5675	Melanoma	True
M28	1.0822	0.58056	0.762	8.2754	5.98377	Melanoma	True
M29	1.53224	0.366149	0.338666	8.38418	6.38995	Melanoma	True
M30	1.45863	0.46469	0.762	8.5561	6.60178	Melanoma	True
M31	1.2779	0.3193	0.8466	8.7209	6.47702	Melanoma	True
M32	2.0909	0.53348	0.67733	8.2525	7.2364	Melanoma	True
M33	1.87795	0.30968	0.762	8.0234	6.8654	Melanoma	True
M34	2.11231	0.3456	0.67733	10.211	8.2249	Melanoma	True
M35	2.1344	0.51591	0.6773	6.2636	6.29687	Melanoma	True
M36	3.8996	0.30355	0.42333	9.7424	10.1828	Melanoma	True
M37	2.7	0.37935	0.84666	10.648	9.2953	Melanoma	True
M38	1.0633	0.28073	0.8466	5.6442	4.6558	nonMelanoma	False
M39	1.59092	0.3677	0.762	6.6709	5.8214	Melanoma	True
M40	1.6759	0.5344	0.67733	8.8994	7.0205	Melanoma	True
M41	1.35253	0.59503	0.8466	8.6623	6.57231	Melanoma	True
M42	4.87195	0.52492	0.508	12.665	12.9727	Melanoma	True
M43	0.8891	0.38835	0.592667	4.3376	3.659841	nonMelanoma	False
M44	0.7351	0.32502	0.67733	3.9933	3.3234	nonMelanoma	False
M45	0.6939	0.34828	0.508	5.5841	3.98296	nonMelanoma	False
M46	0.67751	0.33358	0.67733	4.2317	3.36867	nonMelanoma	False
M47	2.889956	0.37827	0.84666	9.7890	9.1126	Melanoma	True
M48	1.72453	0.37063	0.42333	5.9434	5.46235	Melanoma	True
M49	0.53049	0.26584	0.762	4.6087	3.40158	nonMelanoma	False
M50	0.37748	0.32287	0.762	6.309	4.5856	nonMelanoma	False
M51	3.36769	0.90999	0.84667	9.6028	9.79373	Melanoma	True
M52	2.05317	0.51854	0.84667	7.2833	6.78598	Melanoma	True
M53	1.4103	0.35524	0.67733	5.5703	5.08277	Suspicious	True
M54	2.55615	0.3695	0.84667	11.533	9.5888	Melanoma	True
M55	4.20147	0.37397	0.67733	15.1418	13.4088	Melanoma	True
M56	3.3434	0.52803	0.508	11.2553	10.2809	Melanoma	True
n1	1.1293	0.4879	0.8466	4.4466	4.1635	nonMelanoma	True
n2	0.8825	0.3971	0.4233	4.1856	3.4915	nonMelanoma	True
n3	1.289	0.4916	0.33866	4.4487	4.1186	nonMelanoma	True
n4	1.3262	0.5102	0.762	4.3599	4.3361	nonMelanoma	True
n5	2.0073	0.3438	0.254	4.7662	5.1541	Suspicious	True
n6	1.4334	0.3502	0.6773	4.0022	4.2383	nonMelanoma	True
n7	1.2314	0.698	0.67733	4.5187	4.2687	nonMelanoma	True
n8	1.1385	0.4776	0.6773	4.5438	4.1355	nonMelanoma	True

n9	0.86459	0.4748	0.4233	4.2077	3.487	nonMelanoma	True
n10	0.7568	0.3235	0.33867	5.1856	3.7784	nonMelanoma	True
n11	1.8939	0.5105	0.33866	6.702	6.0338	Melanoma	False
n12	1.01	0.4391	0.67733	5.7639	4.5781	nonMelanoma	True
n13	0.9278	0.3804	0.3386	4.925	3.8765	nonMelanoma	True
n14	0.8765	0.3824	0.4233	4.5722	3.6755	nonMelanoma	True
n15	1.6087	0.4672	0.4233	6.2443	5.4715	Melanoma	False
n16	0.6174	0.4942	0.3386	4.9901	3.5165	nonMelanoma	True

Performance of Proposed approach: In medical Prediction, Sensitivity and Specificity are used to measure the performance of system using the following measures.

- ✓ Data sample which is infected and had a melanoma “positive” test result is termed a true positive (A),
- ✓ Data sample which is infected and had a melanoma “negative” test result is termed a false negative (C)
- ✓ Data sample which is not infected and had a melanoma “positive” test result is termed a false positive (B).
- ✓ Data sample which is not infected and had a melanoma “negative” test result is termed a True negative (D).

The summary of the above are shown in Table 5.3.

Sensitivity, equation (1) is the true positive test results divided by the entire infected cell. This is the probability that the data sample will be classified as positive, when data image is infected.

$$Sensitivity = (A / (A + C)) \dots\dots (1)$$

The specificity, equation (2) of a test is the true-negative test results divided by most the cell that are not infected. This is the probability that data sample will be classified as not infected when sample is negative. “1-specificity is the probability that sample will be classified as positive when the sample data not infected.

$$Specificity = (D / (B + D)) \dots\dots (2)$$

The values of True Positive, False Positive, False Negative and True Negative obtained by actual experimentation are tabulated in table 5.4

Table 5.3: The Definition of True Positives/Negatives

	Infected (+)	Not Infected (-)
Result Positive	A = true positive	B = false positive
Result Negative	C = false negative	D = True Negative

Table 5.4: The values of True Positives/Negatives

	Infected (+)	Not Infected (-)
Result Positive	A = 45	B = 2
Result Negative	C = 11	D = 14

The accuracy of the predictions is measured by the number of correctly predicted cases divided by all the cases in the study (Percent Accuracy). The values obtained by experimentation for Sensitivity and Specificity are 0.80 and 0.87 respectively. Authors found that the matching program system performed 83.00% in detecting the Melanoma skin cancer. The result of the experiment, number of investigated samples and results using the Dermoscopic investigation were 73 and the result using the system was found 60 and 13 were resulted in unmatched with the samples stored. The problem of undetermined skin lesion, and we found that the system is sensitive to the differences of skin lesion.

Further, the automated diagnostic detection were able to predict the malignant melanoma with an accuracy of 60-83% based on selected dependent variables, validated using ROC characteristics which is as shown in figure 5.4. Diagnostic models were developed to predict the skin lesion digital images that are infected with malignant melanoma. The proposed model with variable shows an excellent performance value of the ROC of 0.8166 and 0.8209. ROC can range between 0 and 1 with higher values indicating better performance.

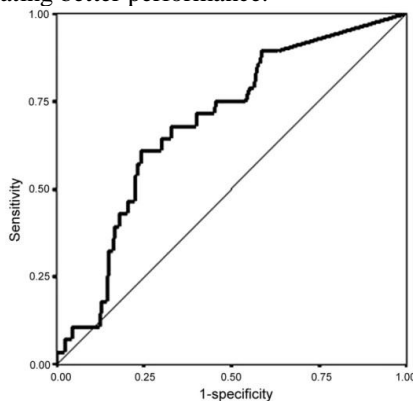


Fig 5.4: ROC Curve

VI. CONCLUSIONS

This section presents a conclusion for the research and ideas for further research. The discussion starts with an introduction to the research achievements, research framework summaries, research work summaries, and the contribution of the research. The discussion ends up with the ideas for future works.

A. Conclusion

Everything that is newly invented has its merits and demerits. The assessment of the newly invented thing is, perhaps, the most crucial phase in not just the invention process, but also in the decision of retaining it as useful, or in proposing to bring in modifications to improve the performance or discarding it as unworthy. However, in fields where robust and/or credible methodologies are already existent, a new approach introduced should not only be entirely assessed, but it should also be thoroughly compared with the existing ones. This gives a clear picture of not only how good the new approach is, but also if it is worthwhile pursuing improvements over the methodology, and also where the approach stands against the state of the art. Newly proposed approach should closely follow the already existing robust ones, and be preferably even better. This is the surest way of bringing in any kind of credibility to the approach right in its inception. The following sections might be of use in assessing new approaches that we have taken up in our research work.

Melanoma skin cancer incident rates have been significantly rising since last two decades. Therefore, early, fast and effective detection of skin cancer is mandatory. If detected at an early stage, skin has one of the highest cure rates, and the most cases, the treatment is quite simple and involves excision of the lesion. Moreover, at an early stage, skin cancer is very economical to treat, while at a late stage, cancerous lesions usually result in near fatal consequences and extremely high costs associated with the necessary treatments.

A Computational vision system for skin cancer detection system is proposed in this paper. System proves to be a better diagnosis method than the conventional Biopsy method. Computer based skin cancer detection is more advantageous to patients, by which patients are possible to detect the skin cancer without going to hospital or without the help of a lab technicians. The proposed model saves a huge amount of time in diagnosing patients. The diagnosing methodology uses DIP Techniques and ABCD rule for the classification and recognition of Malignant Melanoma from benign melanoma. Dermoscopic images were collected and are processed by various Image processing techniques. The unique features of the segmented images were extracted using Hog descriptors and analyzed ABCD rule. Based on the features, the images were classified as Malignant or Benign. The classification system has good accuracy of 83%. Suggested by varying the Image processing techniques and Classifiers of the artificial intelligent techniques, the accuracy of the system can be improved to a greater level.

B. Future Research Avenues

Authors discover that the hybrid model is able to detect the malignant melanoma images with an accuracy of 60.33%-83% based on selected variables. The results of this model are significant, this approach experimented and the results obtained in this research could be useful in determining potential treatment methods and monitoring the progress of treatment for Malignant affected patients.

The feature extraction and classification algorithm are sensitive for to malignant phase wise features that the results such as, using different types of features in malignant diagnosis (color, shape and size) with and using different resolutions. The system performance can be further improved by considering the large image size, and color scaling, and depth. In this experiment the size and color depth of the stored images in the database was 65x65 pixels image size and 8 bit quantization still there is a room for research. The proposed system is sensitive to difference of melanoma phases, due to this reason; it is possible to extend and explore the proposed techniques to diagnose different types of disease.

Using different types of phase melanoma with different geometry and resolution generates a high noise, therefore the types of phase melanoma with different geometry and resolution must be equal in both stored and investigated samples. Further, avenue to design and develop a method(s)/ technique(s) to reduce noise as a follow up to our research work. Finally we would venture the experimenting by incorporating the novel artificial intelligent techniques and expert systems in the proposed in an improved efficient system to diagnose the patients symptoms and then possible to investigate patients' clinical sample.

- i. The numbers of stored samples in the database is small because of unavailability of all kind of samples due to the time scale of the project.
- ii. The problem of undetermined melanoma phases.
- iii. Upon the analysis of the result obtained, we have reached is a considerable state of attempt to build a complete computerized diagnostic vision based system to melanoma disease; same may be extended using the same technique to diagnosis different type of similar diseases such as malaria and other infectious diseases.
- iv. Collaboration establishment with MRI data centers, as clinical data are private property and are confidential, not easily available for research.

ACKNOWLEDGMENT

We have been fortunate in our collaborative efforts with clinical expert District Regional Office, Mandya and Mysore, Karnataka state, India, who not only shared their vast experience in cases of skin cancer in general and by playing the role of advisor but also provided the means to access fewer data for our experiment. As a part of Royal Research Foundation acknowledge and would like to continue to explore possible solutions in collaboration with the clinical experts for the initiation of the Melanoma research. We have been fortunate in our collaborative efforts with clinical expert along with a professional support and valuable assistance from **Dr. Kanthesh B.M.** Assistant Professor of Molecular Biology, Faculty of Life Sciences, JSS University, Mysore India and **Dr. Ganiga Srinivasaiah Sridhar**, Department Of Medicine, Faculty Of Medicine, University of Malaya, Malaysia, who not only shared their vast experience in cases of Malignant Melanoma and by playing the role of advisors for our experiment.


REFERENCES

- [1] Moataz Aboras, Hani Amasha, Issa Ibraheem, "Early detection of melanoma using multispectral imaging and artificial intelligence techniques" *American Journal of Biomedical and Life Sciences* , 29-33, 2015.
- [2] A. Papastergiou, a. Hatzigaidas, z.Zaharis, G. Tryfon, k. Moustakas, d. Ioannidis "Introducing Automated Melanoma Detection in a Topic Map Based Image Retrieval System" *Proceedings of the 6th WSEAS International Conference on Applied Computer Science, Hangzhou, China, April 15-17, 2007.*
- [3] Ilias Maglogiannisa, Dimitrios I. Kosmopoulosb, "Computational vision systems for the detection of malignant melanoma" *oncology reports* 15: 1027-1032, 2006.
- [4] Jamilu Awwalu, Ali Garba Garba, Anahita Ghazvini, and Rose Atuah (2015) "Artificial Intelligence in Personalized Medicine Application of AI Algorithms in Solving Personalized Medicine Problems", *International Journal of Computer Theory and Engineering*, Vol. 7, No. 6, December 2015.
- [5] Omar Abuzagheh , Miad Faezipour and Buket D. Barkana "Skincure: an innovative smart phone-based Application to assist in melanoma early Detection and prevention" *Signal & Image Processing : An International Journal (SIPIJ)* Vol.5, No.6, December 2014.
- [6] S.N. Deepa and B. Aruna Devi "A survey on artificial intelligence approaches for medical image classification", *Indian Journal of Science and Technology*, Vol. 4 No. 11, Nov 2011.
- [7] Ammara Masood and Adel Ali Al-Jumaily "Computer Aided Diagnostic Support System for Skin Cancer: A Review of Techniques and Algorithms" *Hindawi Publishing Corporation International Journal of Biomedical Imaging* Volume 2013, Article ID 323268, 22 pages.
- [8] Maciej Ogorzałek, Leszek Nowak, Grzegorz Surowka and Ana Alekseenko "Modern techniques for computer aided melanoma diagnosis", *Melanoma in the clinic - Diagnosis, Management and Complications of Malignancy* 2011.
- [9] Arthur Tenenhaus "Detection of melanoma from dermoscopic images of naevi acquired under uncontrolled conditions" *PubMed, Skin Res Technol*, 2010 Feb;16(1):85-97.
- [10] A. Abu-Hanna, P. J. F. Lucas. (2001) "Prognostic Models in Medicine" *Methods of Information in Medicine*, © Schattauer GmbH, 1-5, 2001.
- [11] Mehl T, Binder M, Scheibboeck C, Holub S, Adlassnig K-P, Thomas Mehl "Integration of clinical decision support into a hospital information system to Predict metastatic events in patients with melanoma", Schreier G, Hayn D, Ammenwerth E, editors. *Tagungsband der eHealth2010*, Wien: Österreichische Computer Gesellschaft; 2010. p. 107-112.
- [12] Catarina Barata Jorge S. Marques Jorge Rozeira "Detecting the Pigment Network in Dermoscopy Images: a Directional Approach", *Conference proceedings: Annual International Conference of the IEEE Engineering in Medicine and Biology Society. IEEE Engineering in Medicine and Biology Society. Conference*, Aug 2011.
- [13] Harald Ganster, Axel Pinz, Reinhard Röhner, Ernst Wildling, Michael Binder, and Harald Kittler "Automated Melanoma Recognition" *IEEE transactions on medical imaging*, vol. 20, no. 3, march 2001.
- [14] I. Maglogiannis, S. Pavlopoulos, D. Koutsouris, "An Integrated Computer Supported Acquisition, Handling and Characterization System for Pigmented Skin Lesions in Dermatological Images" *IEEE Trans. Inf. Technol. Biomed.*, vol. 9, no. 1, pp. 86-98, 2005.
- [15] Zhenghao Shi1, and Lifeng He (2010) "Application of Neural Networks in Medical Image Processing", *Proceedings of the Second International Symposium on Networking and Network Security*, April. 2010.
- [16] Paulo J. Lisboa , Azzam F.G. Taktak "The use of artificial neural networks in decision support in cancer: A systematic review", *Neural Networks* 19, 408-415, 2006.
- [17] Hussain, W., W. Ishak, F. Siraj. *Artificial Intelligence in Medical Applications: An Exploration*. - In: *National Conference on Management Science: New Paradigm for Knowledge Economy*, University of Malaysia, Serdang, Selangor, 2001. Preprint: *Artificial Intelligence in Medical Application: An Exploration*. *Health Informatics, Europe Journal*, 2002.
- [18] Rajesh Shankarapillai "Periodontal disease risk assessment using Artificial neural networks" Ph.D, Pacific University, 2010.
- [19] AN Ramesh, C Kambhampati, JRT Monson, PJ Drew (2004) "Artificial intelligence in medicine", *Annals of the royal college of surgeons of England*, 334-338, October 2004.
- [20] Konstantin Korotkov "Automatic change detection in multiple pigmented skin lesions", *Artificial intelligence in medicine*. 56, 69-90, 2014.
- [21] Siddiq Iqbal, Divyashree.J.A, Sophia.M, Mallikarjun Mudas, Vidya.R (2015) "Implementation of Stolz's Algorithm for Melanoma Detection" *International Advanced Research Journal in Science, Engineering and Technology* Vol. 2, Issue 6, June 2015.
- [22] Nilkamal S. Ramteke and Shweta V. Jain (2013) *Analysis of Skin Cancer Using Fuzzy and Wavelet Technique – Review & Proposed New Algorithm*, *International Journal of Engineering Trends and Technology (IJETT) – Volume 4 Issue 6- June 2013.*
- [23] Harpreet Kaur Aashdeep Singh (2015) "A Review on Automatic Diagnosis of Skin Lesion Based on the ABCD Rule & Thresholding Method" *International Journal of Advanced Research in Computer Science and Software Engineering*, Volume 5, Issue 5, May 2015.

- [24] D.Saranya, V.Radha (2014) “Melanoma Skin Cancer Detection:A Review” International Journal of advanced studies in Computer Science and Engineering IJASCSE, Volume 3, Issue 8, 2014.
- [25] Sanjay Jaiswar, Mehran Kadri, Vaishali Gatty “Skin Cancer Detection Using Digital Image Processing” International Journal of Scientific Engineering and Research (IJSER) Volume 3 Issue 6, June 2015, 138-140.
- [26] Aswin.R.B, J. Abdul Jaleel, Sibi Salim “Implementation of ANN Classifier using MATLAB for Skin Cancer Detection” International Journal of Computer Science and Mobile Computing, ICMIC13, December- 2013, pg. 87-94.
- [27] Md.Amran Hossen Bhuiyan, Ibrahim Azad, Md.Kamal Uddin “Image Processing for Skin Cancer Features Extraction” International Journal of Scientific & Engineering Research Volume 4, Issue 2, February-2013.
- [28] S. Raviraja, Gaurav Bajpai and Sharma S “Analysis of Detecting the Malarial Parasite Infected Blood Images Using Statistical Based Approach”, Proceedings 15, pp. 502-505, 2007
- [29] S. Raviraja, Geethanjali S.D, C. Chethana, Kanthesh. B.M " The Classification and Recognition of Plasmodium Parasite in Prediction of Malaria infected blood smears using Artificial Intelligence Technique”, International Journal of Advanced Research in Computer Science and Software Engineering, Vol 5, Issue 6, June 2015.
- [30] S. Raviraja, Saif Saeed Osman, Kardman "A Novel Technique for Malaria Diagnosis using invariant moments and by image compression", 4th Kuala Lumpur International Conference on Biomedical Engineering (Biomed 2008) Malaysia. IFMBE Proceedings, the International Federation for Medical and Biological Engineering, ISSN 1680-0737, pp 730-733.

AUTHOR’S PROFILE

 <p>Dr. S. Raviraja, PhD, PDRF., Founder Chairman, Royal Research Foundation, Mysore, India. Former Employee, Post Doctoral Research Fellow, Dept. Of Artificial Intelligence University of Malaya, Kuala Lumpur, Malaysia.</p>	<p>Dr. S. Raviraja, founder of Royal Research Foundation, India, a Research Institute at present and former employee of department of Artificial Intelligence, the Faculty of Computer Science and IT at University of Malaya (UM), Malaysia. Previously he was attached to the Faculty of CS & IT at the University of Medical Sciences and Technology in Sudan. He has received his Bachelors in Computer Science and Masters in Computer Applications from University of Mysore, India. Also he has a PhD from University of Honolulu, US in which he built a multilingual script classification & recognition of African Language Scripts. Also served as Post Doctoral Research Fellow at University of Malaya. This contemporary research from several perspectives (such as image process, robotic/computer vision, 3G mobile application on controlling and monitoring) has met the necessity of addressing many of the theoretical, practical and methodological issues surrounding research on AI.</p> <p>Raviraja has presented his research findings at several national, international conferences, journals, workshops and also has innovation awards to his credit. He has previously taught, examined students of India, Ethiopia, Sudan, Middle East countries, and Malaysia. During his stay at UM he was also actively involved in teaching and supervising undergraduate and postgraduate students. Formerly he was serving Editorial Member of Malaysian Journal of Computer Science (ISI Indexed: ISSN 0127-9084) and ICTACT Journal of Soft Computing (ISSN 0976-6561) etc., He is also member of Institute of Engineers India, Computer society of India and several other professional associations. His research interest includes Medical & Document Image Analysis, DIP, AI & Robotics and in Software Engineering Methodologies.</p> <p>Raviraja started his career with Motorola (India) as Software Engineer, later as Software Analyst and then as Project lead in reputed software companies in India, such as Pentasoft Technologies Pvt Ltd, and Raman InfoTech Ltd. He was then working as a research scholar and later as Assistant Professor university in Ethiopian, few years later continued his academic and research career with university in Sudan working on automated detection of malaria. He also served as dept. Head and Dean of the school in previous institutions. Later, had selection from University of Malaya (Ranked 130 by THES QS 2010) as a Post Doctoral Research Fellow. At present he is a founder chairman of Royal Research Foundation, a research institute in India.</p>
 <p>Manasa E, BE., Research Scholar, (M.Tech) Department of</p>	<p>Manasa E, Student, M.Tech, Department of Computer Science and Engineering, PES College of Engineering, Mandya, India. She has received her Bachelors of Engineering in Computer Science from Visvesvaraya Technological University, Belgaum, India. She is interested in New Innovations and Research in Vision and Intelligence. At present she has submitted her final thesis towards the award of M.Tech degree and working on a Research Project on Image Processing entitled An Automated Diagnosis and Classification of Malignant Melanoma skin cancer using AI Techniques Under the guidance of Dr.S Raviraja, Founder, Royal Research Foundation, Mysore, India. Also she is working as a Research Associate at Royal Research Foundation. Her Research areas of interest includes Image processing, Medical & Document Image Analysis, Computer vision. Currently</p>

<p>Computer Science and Engineering, PES College of Engineering, Mandya. India.</p>	<p>working on newer challenges and opportunities in the area of vision and intelligence towards his doctoral studies.</p>
 <p>Anitha M. L, B.E, M.Sc(Eng) Associate Professor CS & E Department PES College of Engineering, Mandya, Karnataka, India.</p>	<p>Anitha. M .L. received B.E. degree in Computer science from University of Mysore in 1990 and M.Sc(Engg) by research in Computer science from Visveswaraiah Technological University, Belgaum in 2007. Currently working as Associate Professor at Department of Computer Science, P.E.S. College Of Engineering, Mandya, Karnataka.</p> <p>She has more than 18 years of teaching experience. She is also a life member of ISTE and Research areas of interest includes biometrics, data mining, Image processing, Medical & Document Image Analysis, Computer vision. Currently pursuing on newer challenges and opportunities in the area of Biometrics towards her doctoral studies, supervising postgraduate students and has published several research articles.</p>